J. Phys. Chem. A **2006,** *110,* 207−218

Reaction Paths of the [2 + 2] Cycloaddition of X=C=Y Molecules (X, Y = S or O or CH_2). Ab Initio Study

Joanna E. Rode[†] and Jan Cz. Dobrowolski*[,†,‡]

Industrial Chemistry Research Institute, 8 Rydygiera Street, 01-793 Warsaw, Poland, and National Institute of Public Health, 30/34 Chełmska Street, 00-725 Warsaw, Poland

Received: April 29, 2005; In Final Form: November 10, 2005

The reaction paths of [2 + 2] cycloaddition of the X=C=Y cumulenes were modeled at the MP2/aug-cc-pVDZ level. Cycloadditions of allene and CO_2, CS_2, or OCS lead in part to the same four-membered products as dimerizations of either ketene or thioketene or addition of ketene and thioketene, respectively. All the reactions studied are concerted and mostly asynchronous. The majority of the allene cycloadditions studied are endoergic and proceed with much higher activation barriers than do the alternative (thio)ketene additions. In comparison with the energy of the substrates, the four-membered cycles incorporating S-atoms are stabilized more than the analogous structures with O-atoms built into the rings. There are also some products that are thermodynamically disfavored, yet seem to be obtainable thanks to a relatively low barrier of the reaction. The AIM analysis of the electron density distribution in the transition state structures allowed distinguishing pericyclic from pseudopericyclic and nonplanar-pseudopericyclic types of reaction.

Introduction

Four-membered heterocycles are of concern for today's chemistry. Introduction of heteroatoms into a small ring produces significant changes in charge distribution and ring strain of the whole molecule.[1] Usually, heterocyclic four-membered rings are thermally unstable and highly reactive. Therefore, they are desirable products as well as building blocks for further syntheses. 2-Oxetanones (**a**, Scheme 1) considered, inter alia, in this paper have stimulated considerable interest in the pharmaceutical community owing to their potent biological activity spectrum ranging from enzyme inhibition to viral inactivation as well as pancreatic lipase inhibitors, which are supposed to be responsible for obesity.[1] 2-Oxetanones have also been utilized as herbicides and even as educts for preparing polymeric materials.[1] Among 2-oxetanones, diketene (4-methylene-2-oxetanone; **b**, Scheme 1) is a reactive and versatile compound that is used for introducing functionalized C_2, C_3, and C_4 units into organic compounds.[2] Diketene has been also reported to be a potent bactericide useful for disinfecting large areas.[2] 3-Oxetanones (**c**, Scheme 1) also exhibit biological activity.[3] Numerous steroids incorporating the 3-oxetanone ring exhibit anti-inflammatory and anti-glucocorticoid activity, whereas some of them act as oral diuretics.[4] In the presence of a base, 3-oxetanones are unstable and slowly polymerize to give a highly viscous material, presumably polyoxetanone [$-CH_2C(O)-CH_2-O-$].[5]

The chemistry of sulfur analogues of oxetanones has been less developed. However, in the group of compounds, β-propiothiolactones (**d**, Scheme 1) are used in commercial polymerization and also in laboratory preparation of macrocyclic thiolactones which were demonstrated to exhibit supramolecular properties.[6] The isomers of diketene and its sulfur analogue are known, too. The compounds with two heteroatoms built into the ring exhibit interesting properties. The most known are 1,2-dioxetanes (**e**, Scheme 1), whose chemiluminescent properties have found extensive application in emergency lighting, traffic control, and sports products (lightening golf balls, hockey pucks),[7] as well as in bioanalytical and clinical chemistry for the determination of biomolecules, DNA fingerprinting and sequencing, reporter gene assays, virus detection, and microbe screening.[1,8] In the group of compounds with two sulfur atoms built into the ring, substituted 1,3-dithietanes (**f**, Scheme 1), when directly attached, increase the activity of cephalosporins.[1] On the other hand, the 2-ylidene derivative (known as YH439) inhibits the mutagenicity and tumorigenicity of vinyl carbamate in liver; hence it has been proposed as a new hepatoprotective agent.[9] Also, methylene substituted dithietanes are antibiotics active against Gram-negative bacteria, and some of them are claimed to be fungicides and drugs decreasing hyperglycemia. Imino 1,3-dithietanes are very useful synthetic pesticides and fungicides.[1] Many derivatives of 1,3-dithietane are used as plasticizers in the production of poly(vinyl chloride) or as monomers in the preparation of polyester coatings.[1]

A [2 + 2] cycloaddition of π-electron compounds is potentially an attractive, straightforward way for obtaining the four-membered heterocycles (Scheme 2).[1] The ketene [2 + 2] cycloaddition (dimerization), which serves as a kind of reference reaction in this paper, has been studied by both experimental[10] and theoretical[11,12] methods. In 1934, kinetic studies revealed that diketene dimerization does not proceed through a biradical intermediate.[10a] The above was confirmed in 1943 by studies on diketene pyrolysis.[10b] Since the mid-1950s, it has been known that diketene is the main product of the dimerization; however, in the case of dimerization of substituted ketenes, derivatives of cyclobutadione may be the preeminent product.[2] The ketene dimerization activation barrier, found experimentally for the gas phase, is equal to 31 kcal/mol,[10b] and calculated at the SCF/DZ+P level is equal to 32 kcal/mol (probably by chance).[12] 1,3-Cyclobutanedione, a potential ketene dimerization product,

* Corresponding author. E-mail: Jan.Dobrowolski@ichp.pl or janek@il.waw.pl.
† Industrial Chemistry Research Institute.
‡ National Institute of Public Health.

10.1021/jp0522260 CCC: $33.50
Published on Web 12/15/2005

SCHEME 1: Examples of Four-Membered Ring Compounds Important to Pharmacy and Chemical Industry[a]

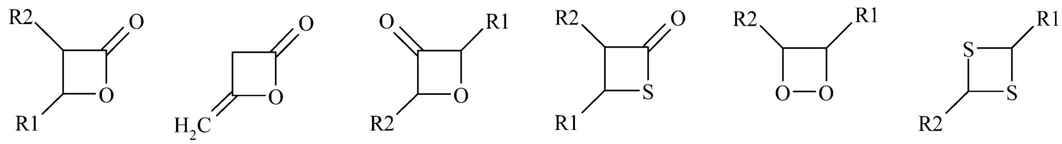

a **b** **c** **d** **e** **f**

[a] Compounds: **a**, 2-oxetanones; **b**, diketene; **c**, 3-oxetanones; **d**, β-propiothiolactones; **e**, 1,2-dioxetanes; **f**, 1,3-dithietanes.

SCHEME 2: Possible Product Structures Obtained from [2 + 2] Cycloaddition of Cumulene Structures Considered

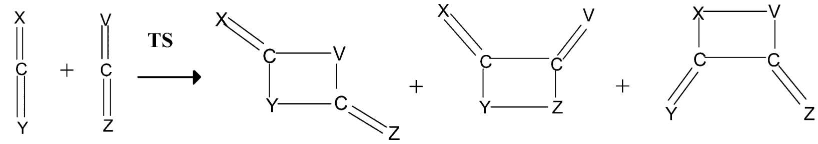

SCHEME 3: Orbital Arrangement of Two Ketene Molecules Allowed by the Woodward−Hoffmann Rules for the [$_{\pi}2_s$ + $_{\pi}2_a$] Cycloaddition Reactions Leading to Diketene (top) and 1,3-Cyclobutadinone (bottom)

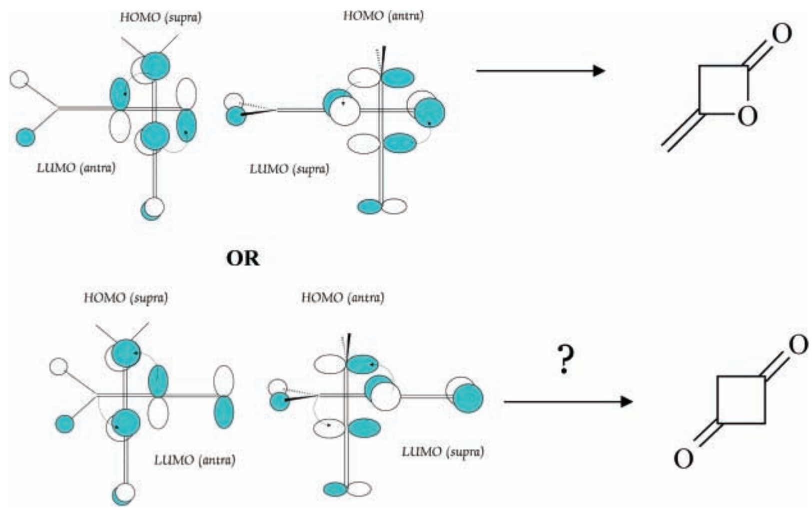

requires a 36 kcal/mol barrier to be overcome[12] and usually is not formed in detectable amounts. The structure of the transition state toward diketene formation, found at the SCF level,[12] indicated a nonsynchronous reaction with partial formation of one σ-bond and partial breakage of two π-bonds. The nonsynchronous reaction mechanism was also calculated for the pathway leading to 1,3-cyclobutanedione, though the product is a symmetrical molecule. The activation barriers for formation of diketene, 1,3-cyclobutanedione, and 2,4-dimethylene-1,3-dioxetane, calculated at the MP2/4-31G* level, were found to be equal to 29.8, 35.1, and 61.2 kcal/mol, respectively.[12] Quite recent studies, performed at the MP2/6-31G*, MP4/6-31G*//MP2/6-31G*, and CCSD(T)/6-31G* levels, yielded transition state (TS) structures fairly similar to that of ref 12; however, the CCSD(T) calculations suggested 1,3-cyclobutanedinone to be the main product favored by the lowest reaction energies of both the ground and TS states.[13] It seems that, until now, the mechanism of the diketene formation has not been established unequivocally.

The early reaction mechanism concepts were based on the Woodward−Hoffmann (W−H) orbital symmetry conservation rules.[14] To apply the rules, there must be a symmetry element intersecting the newly forming bonds and the process must be concerted (i.e., must proceed in one step). The W−H rules have recently been criticized.[15−17] If one molecule is in an excited state, it is geometrically different from the other, the system loses symmetry, and the rules are no longer valid.[15] Studies on the simplest example for which the *supra*−*antra* [$_{\pi}2_s$ + $_{\pi}2_a$] mechanism must be obeyed, the ethene cycloaddition, show that this is a stepwise (i.e., multistep) reaction rather than a concerted process.[16] Moreover, an attempt to find the ethene cycloaddition transition state corresponding to the [$_{\pi}2_s$ + $_{\pi}2_a$] mechanism has failed: instead of first order, the second-order saddle point was found to occur at the MC-SCF level.[17] Although the presence of a heteroatom excludes the existence of a symmetry element intersecting the newly forming bonds, for the ethene−ketene and ketene−ketene [2 + 2] cycloadditions, Woodward and Hoffman had proposed the [$_{\pi}2_s$ + $_{\pi}2_a$] mechanism.[14] According to the rules, in the ketene dimerization the two ketene molecules should be placed either in parallel or in perpendicular planes (Scheme 3). For the ketene dimerization, attempts at finding the TS structures meeting the W−H rules has failed.[12] In the pathway leading to 1,3-cyclobutanedinone, the structures corresponding strictly to the rules for the [$_{\pi}2_s$ + $_{\pi}2_s$] addition, possessing C_{2h} symmetry, exhibited four imaginary frequencies instead of one characterizing TS, whereas the structure corresponding to the [$_{\pi}2_s$ + $_{\pi}2_a$] pathway exhibited two imaginary frequencies.[12] Therefore, for ketene dimerization, the [$_{\pi}2_s$ + $_{\pi}2_s$ + $_{\pi}2_s$] concerted pathway with three π-bonds incorporated and unsymmetrical TS has been recognized.[12,18]

Now, the cycloaddition reactions are analyzed in terms of pericyclic and pseudopericyclic types of reaction rather than the Woodward−Hoffmann rules.[14] The W−H rules were formulated only for pericyclic reactions. A pericyclic reaction is concerted and takes place on a closed curve.[14] The transition structures of pericyclic reactions are expected to be highly nonplanar.

According to the original Ross, Seiders, and Lemal's papers[19] in which the term "pseudopericyclic reaction" was introduced, "a pseudopericyclic reaction is a concerted transformation whose primary changes in bonding compass a cyclic array of atoms, at one (or more) of which nonbonding and bonding atomic orbitals interchange roles. In a crucial sense, the role interchange means a 'disconnection' in the cyclic array of overlapping orbitals because the atomic orbitals switching functions are mutually orthogonal". In that paper,[19a] a [1,3] sigmatropic reaction was analyzed and a lone pair was transformed into a single bond, and at the same time another single bond was transformed into another lone pair. This occurred in a "cyclic array of atoms".

For nearly 20 years, pseudopericyclic reactions did not attract much attention. In the mid-1990s Birney first,[20] and later several other authors,[21−25] revived their interest in them and showed that a number of organic syntheses follow this type of process. Birney and co-workers concluded that in the pseudopericyclic reactions the TS structure (1) is planar (or nearly planar), (2) exhibits orbital disconnections, and (3) determines relatively low activation barrier; additionally, (4) pseudopericyclic reactions are orbital symmetry allowed.

The pseudopericyclic reaction is studied by using two main treatments: the atomic and molecular orbital formalism [Lemal,[19] Birney[20]] and the electron density concept [Chamorro,[24] Lopez[25]]. In 2003, Chamorro used the electron localization function (ELF) method to study exactly the same reactions as Birney,[20b] in which atomic and molecular orbital methodology was used. The conclusions of both studies were identical. It is crucial that, in the ELF methods, the concept of "disconnection" involved in an orbital framework was replaced by detecting disconnections via examination of direct electron fluctuation at the interaction centers.

The atoms-in-molecules (AIM) method used in this paper is equivalent to the ELF method used by Chamorro. A minor difference between the methods consists of the fact that, in the AIM theory, electron density basins are associated with "atoms", whereas in the ELF approach they are associated with "pair regions". The absence of a bond in the AIM method is connected to the lack of the bond critical point (BCP), whereas in the ELF method negligible electron exchange between the basins is associated with appropriate "pair regions".

Quite recently, López et al.[25] have used successfully AIM analysis to study pericyclicity and pseudopericyclicity of electrocyclic reactions. In particular, López et al. showed the ellipticity of the BCP to be a very useful tool in classification of the reaction mechanisms. As stated by López et al.,[25] electron density is a physical observable; therefore, by using them one avoids any arbitrary processing of the wave functions such as orbital localization (and replacement of molecular orbitals by an arbitrary and illustrative, yet oversimplified, atomic orbital picture). It is also thought that the analysis based on the localized orbitals may not be fully adequate to describe TS structures whose orbitals are essentially diffused.

It can be summarized that, until now, to differentiate the pseudopericyclic from the pericyclic type of reactions, the following approaches were used: the natural bond analysis (NBO) of the TSs,[20,21] magnetic properties and aromaticity of the TSs,[22,23] anisotropy of the current induced density (ACID) analysis,[23] electron localization function (ELF),[24] and ellipticity of AIM determined critical points.[25]

Motivation for the present study originates from contemplation of a potential applicability of CO_2, the industrial waste and pollutant, addition to allene ($CH_2{=}C{=}CH_2$) that would lead to the industrially desirable product: diketene. The reaction was found to be thermodynamically disfavored.[26] However, it is known that, at high pressure of H_2 and in the presence of a $[RhCl(C_2H_4)(P^iPr_3)]_2$ catalyst, 3-methylene-2-oxetanone is formed from CO_2 and allene.[27] Thus, the reaction barrier appeared to be substantial, and the present study stems from this very problem. Because thioketene was reported to be even more reactive than ketene,[28] we extended the study to cover sulfur analogues of CO_2 and ketene cycloaddition reactions. In fact, we consider cycloaddition leading to all possible four-membered cycle product molecules containing two heteroatoms, either O or S or both. To this aim, we performed the MP2/aug-cc-pVDZ calculations of the reactants, TS structures, and reaction products. The atoms-in-molecules (AIM)[29] analysis of critical points of the electron density in the TSs allowed us to find arguments for a distinction between pericyclic, pseudopericyclic, and nonplanar (NP)-pseudopericyclic type of reactions.

This paper is organized as follows: First, we compare the [2 + 2] addition reaction of CO_2 and allene with ketene dimerization. Second, the analogous comparison is made for the CS_2 and thioketene reactions. Third, the OCS and allene additions are compared with the additions of thioketene and ketene. Next, the energetic and geometry regularities are summarized. Finally, reaction mechanisms are discussed in terms of the AIM method.

Calculations

The ab initio MP2/aug-cc-pVDZ calculations[30,31] were performed by using Gaussian 98 and Gaussian 03 packages of programs.[32] The transition structures were found by using the quadratic synchronous transit-guided quasi-Newton (QST3) method developed by Schlegel and co-workers, which uses a quadratic synchronous transit approach to get closer to the quadratic region around the transition state, and then uses a quasi-Newton or eigenvector-following algorithm to complete the optimization.[33] As for minimizations, it performs optimizations by default by using redundant internal coordinates.[34] For the lowest reaction barriers the intrinsic reaction coordinate (IRC) calculations[35] were performed for both the forward and reverse directions of the vibrational mode calculations to confirm that the transition states found connect the appropriate minima.

The G3 method[36] was used when the energies of two structures were almost equal. The G3 calculations are composed of several stages (the MPBT calculations corrected for a spin−orbit term and some higher level corrections for valence electrons) and were shown to yield energy accuracy of 1−2 kcal/mol.[36]

The imaginary vibrations were visualized by using the Molekel 4.0 program.[37] The bond critical points (3,−1) and the ring critical points (3,+1) in the TS structures were localized by using the AIM2000 program.[29a]

Results and Discussion

The [2 + 2] cycloaddition of allene and CX_2 (path A) and the H_2CCX dimerization (path B) can lead potentially to two and six products, respectively (Figures 1 and 2). The [2 + 2] cycloaddition of allene and OCS (path A) and the H_2CCO addition with H_2CCS (path B) can lead potentially to four and eight products, respectively (Figure 3). The Gibbs free energy differences, defining the reaction energies and the activation barriers at 298 K, are presented in Chart 1 (CO_2 + allene vs ketene + ketene), Chart 2 (CS_2 + allene vs thioketene + thioketene), and Chart 3 (OCS + allene vs ketene + thioketene). Schematic structures, molecule numbering, and names are listed

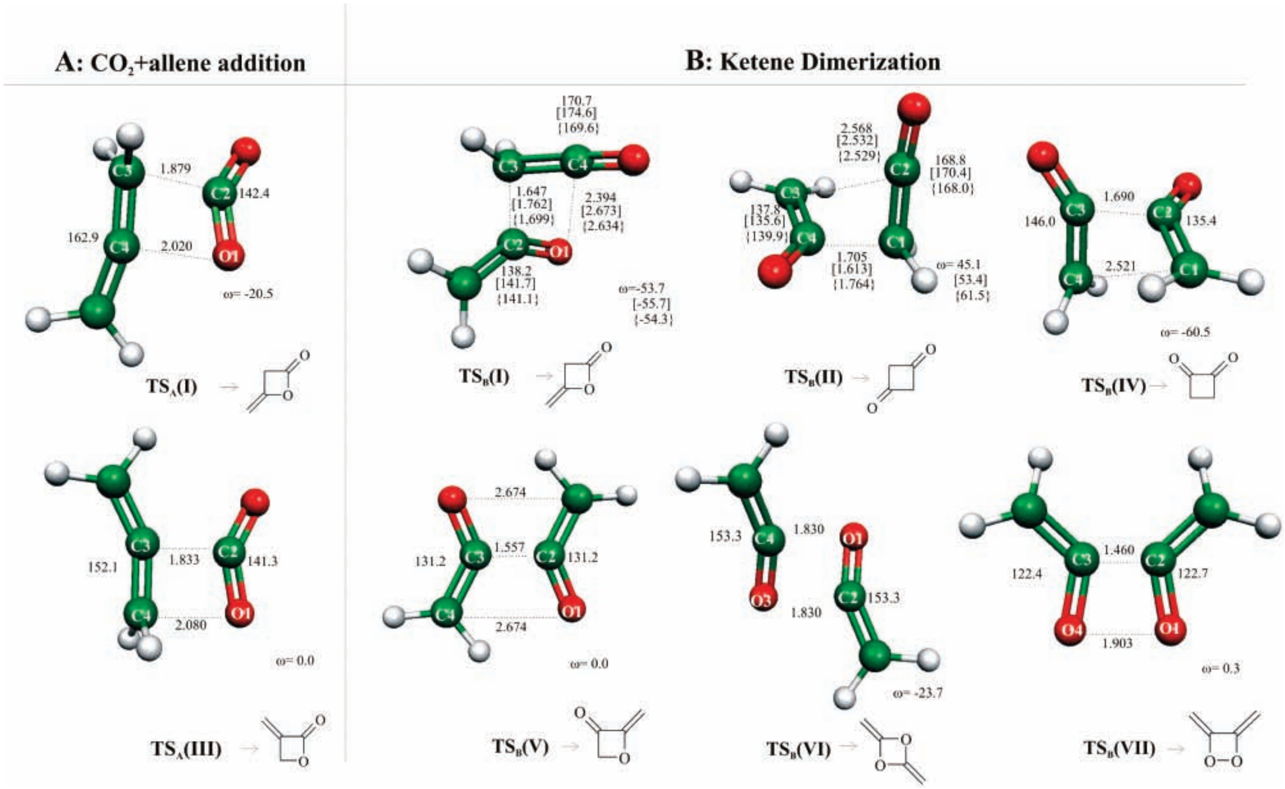

Figure 1. Atom numbering and selected geometric parameters (angstroms and degrees) of the transition state structures for CO_2 and allene cycloaddition (path A) and ketene dimerization (path B) calculated at the MP2/aug-cc-pVDZ level of theory. Values in brackets and braces are taken from refs 12 and 13, respectively.

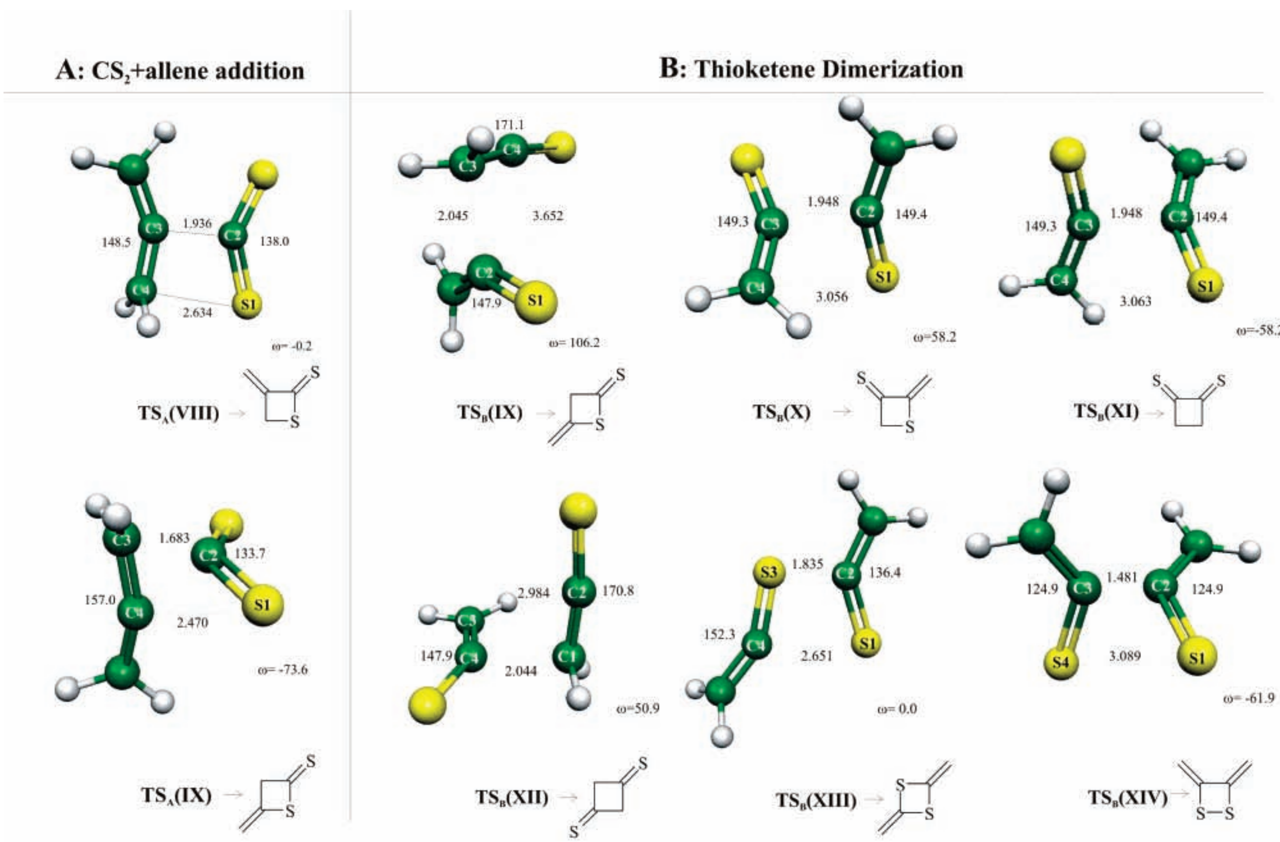

Figure 2. Atom numbering and selected geometric parameters (angstroms and degrees) of the transition state structures for CS_2 and allene cycloaddition (path A) and thioketene dimerization (path B) calculated at the MP2/aug-cc-pVDZ level of theory.

in Table S1 of the Supporting Information (SI). The HOMO–LUMO orbital energy gaps for the reactants studied are gathered in Table S2 of SI. All the energetic data are collected in Tables S3, S4, and S5. They contain also the energetics at 0 K corrected for zero-point energies, and mode specification of imaginary frequencies at the transition states. Additionally, the geometric

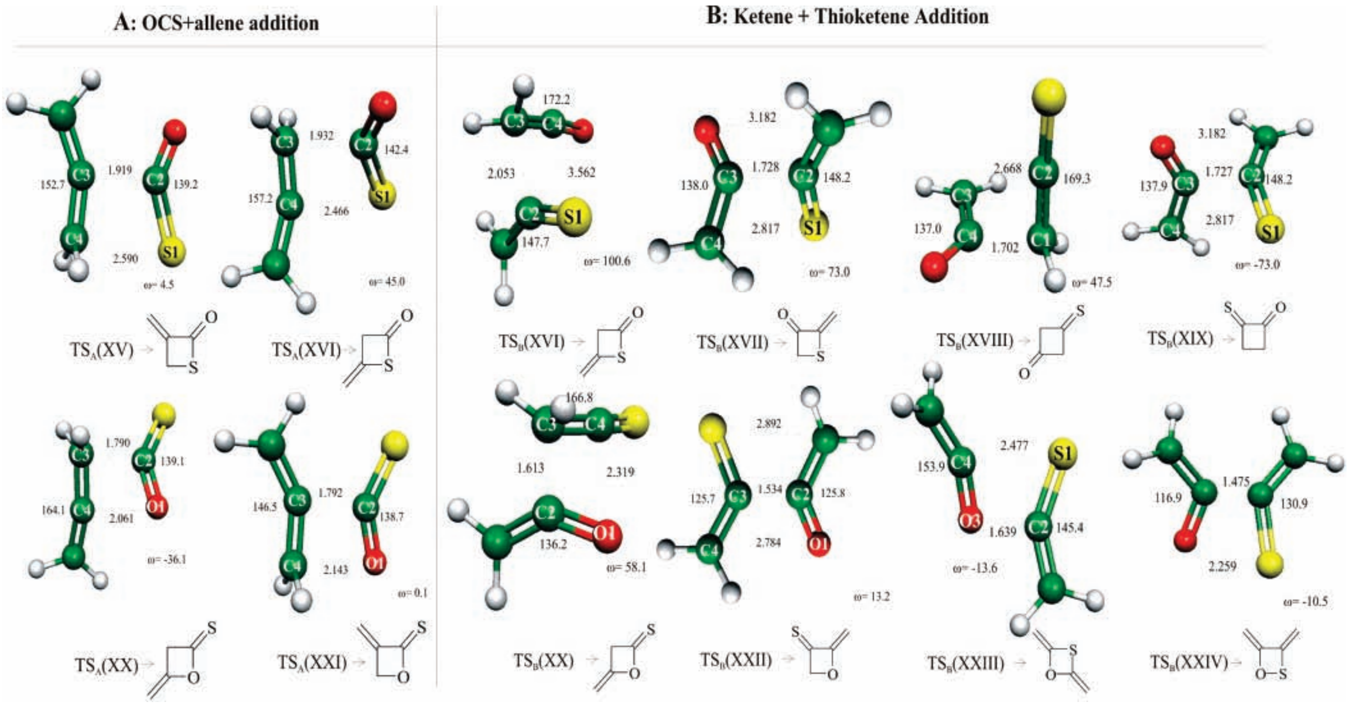

Figure 3. Atom numbering and selected geometric parameters (angstroms and degrees) of the transition state structures for OCS and allene cycloaddition (path A) and cycloaddition of ketene with thioketene (path B) calculated at the MP2/aug-cc-pVDZ level of theory.

CHART 1: Energetics ΔG (p = 1 atm, T = 298 K) of the [2 + 2] Cycloaddition Reaction of Allene and CO_2 (Path A) and Ketene Dimerization (Path B) Calculated at the MP2/aug-cc-pVDZ Level[a]

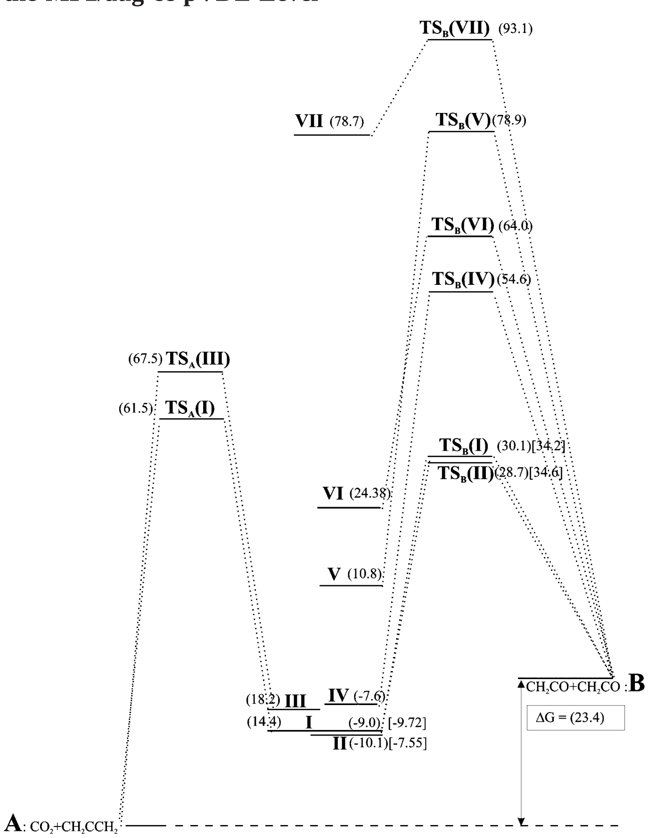

[a] The G3 energies are presented in brackets. For numbering of the structures, see Figure 1.

details and energetic data on the products and transition states studied are collected in Tables S6−S11 of SI.

Allene Addition to CO_2 vs Ketene Dimerization. Some products of the CO_2 addition to allene, as well as ketene dimerization reaction (Figure 1), were studied by us previously.[26] Therefore, we place here special emphasis on the transition states. Hereafter, the ω-angle reflects the deformation of the four-membered ring and is defined as the dihedral angle of the 1−2−3−4 ring atoms.

The previous studies on ketene dimerization[12,13] have shown that the energy difference between the most stable products **I** (diketene) and **II** (1,3-cyclobutanedione) is very sensitive to the computational method applied. This also holds true in our calculations. At the MP2/aug-cc-pVDZ level, structure **II** seems to be favored both thermodynamically and kinetically, although the energy difference between the molecules **I** and **II** equals ca. 1 kcal/mol, a value within the range of accuracy of the computational method used. The activation barrier for **I** is equal to 30.1 kcal/mol and it is in very good agreement with the experimental value (31 kcal/mol),[10b] however; in contrast to the experimental findings, the barrier calculated for **II** is lower than that for **I** by 1.4 kcal/mol. The reaction paths toward **I** and **II** were confirmed by the IRC calculations (Figure S1). To verify the magnitude of the TS energy difference, we recalculated the structures by using the G3 method constructed specially for reaction energetics. As a result, the barrier toward **I** was lower than that toward **II**, yet the experimental values were reproduced less accurately than those at the MP2/aug-cc-pVDZ level. Surprisingly, the CCSD(T)/6-31G* calculations, assumed to be accurate, have favored formation of **II**, whereas CCSD/6-31G* and CASSCF have favored **I** by a lower activation barrier.[13]

The third, still thermodynamically stable product of ketene dimerization, **IV** (1,2-cyclobutanedione), has never been reported, yet, the unstable product **VI** (2,4-dimethyleno-[1,3]-dioxetane) was a subject of theoretical study[11c] and was shown to be by 30 kcal/mol less stable than **I** and **II**. Although **IV** is expected to be stable (Chart 1, Tables S3 and S7), the activation barrier leading to **IV**, TS_B(**IV**), is almost twice as high as TS_B(**I**) and TS_B(**II**). The other ketene dimerization products are

CHART 2: Energetics Δ*G* (*p* = 1 atm, *T* = 298 K) of the [2 + 2] Cycloaddition Reaction of Allene and CS_2 (Path A) and Thioketene Dimerization (Path B) Calculated at the MP2/aug-cc-pVDZ Level[a]

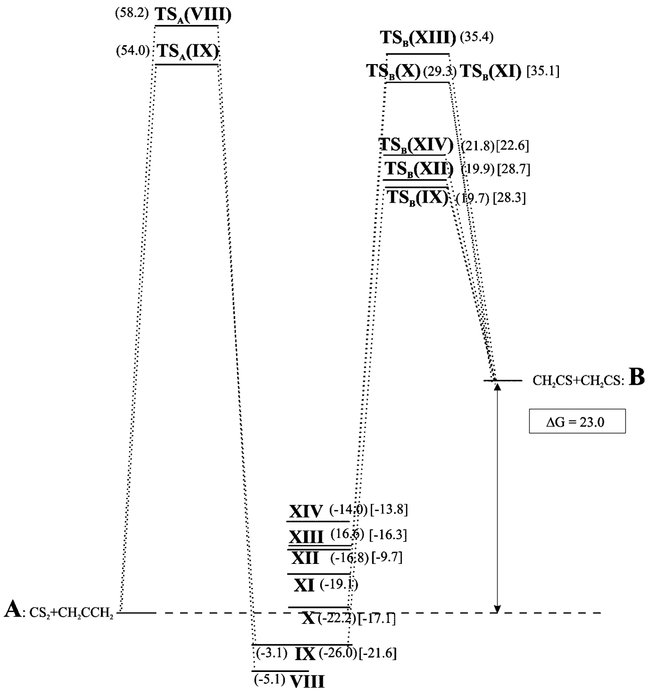

[a] The G3 energies are presented in brackets. For numbering of the structures, see Figure 2.

CHART 3: Energetics Δ*G* (*p* = 1 atm, *T* = 298 K) of the [2 + 2] Cycloaddition Reaction of Allene and OCS (Path A) and Cycloaddition of Ketene with Thioketene (Path B) Calculated at the MP2/aug-cc-pVDZ Level[a]

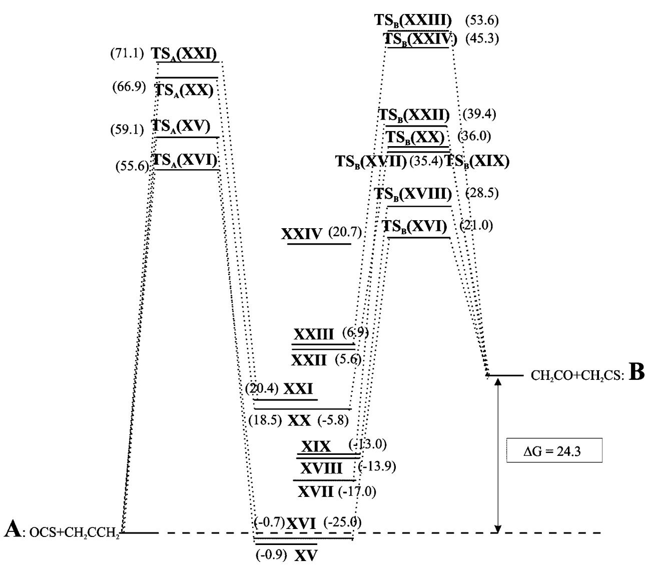

[a] For numbering of the structures, see Figure 3.

both thermodynamically unstable and have high activation barriers. The least stable is **VII** (3,4-dimethyleno-[1,2]-dioxetane), with TS energy high enough to excite one of the ketene molecules to the triplet state during dissociation into two ketenes. The possibility of such an excitation is common to the class of such compounds.[38]

Most of the ketene dimerization reactions are concerted, although they proceed through the TS geometries suggestive of a highly nonsynchronous process (Figure 1). Always the *σ*(C−C) bond is formed first and the *σ*(C−O) next, though the latter is shorter in the product. In TS structures, the differences between *σ*(C−C) and *σ*(C−O) distances exceed 0.6 Å (Table S6). However, TS_B(**VI**) constitutes an exception: the two *σ*(C−O) bonds are formed simultaneously. In this case, the two ketene molecules approach each other in nearly the same plane, the TS_B(**VI**) is skewed by $\omega = 24°$, and the product belongs to the C_{2h} symmetry point group. Also TS_B(**V**) and TS_B(**VII**) belong to the C_{2h} and C_s groups, respectively.

Lack of symmetry of the TS_B(**I**), TS_B(**II**), and TS_B(**IV**) is counterintuitive, because the products belong (nearly) to the C_s, D_{2h}, and C_{2v} point groups of symmetry, respectively. This results from the way the molecules approach each other: first, the heavy atoms are not in one plane; second, the planes determined by the $=CH_2$ groups are close to perpendicular. It is noticeable that at the same time these asymmetric TS structures have relatively low energies. Moreover, comparison of the reactants' original geometries shows one of them to be deformed only slightly. Generally, the geometries of TS_B(**I**) and TS_B(**II**) calculated here are quite similar to those calculated previously by using the HF and MP2 methods.[12,13] However, as can be expected, the agreement with the MP2/6-31G* results[13] is better than that with the HF/DZ+P data.[12] The previous studies have concluded the ketene dimerization to run by the concerted $[_\pi 2_s + _\pi 2_s + _\pi 2_s]$ mechanism[12] instead of the $[_\pi 2_s + _\pi 2_a]$ predicted by the Woodward−Hoffmann rules.[14] The W−H rules require one symmetry element to be preserved throughout the entire reaction path, whereas such a constraint leads to the C_2 symmetry stationary point of second order.[12] Thus, interaction of three *π*-bonds was proposed for the TS_B(**I**): HOMO and LUMO of one molecule and HOMO of the other.[12] The AIM analysis of critical points in the TSs (presented in more detail in The [2 + 2] Cycloaddition Mechanisms section) suggests, however, that the reaction with TS_B(**I**) is pseudopericyclic rather than pericyclic. Thus, neither $[_\pi 2_s + _\pi 2_a]$ nor $[_\pi 2_s + _\pi 2_s + _\pi 2_s]$ mechanisms can obey for the reaction since the W−H rules cannot be applied for pseudopericyclic reactions.

The reaction that would lead also to the diketene molecule **I** is [2 + 2] cycloaddition of allene to CO_2. Then, the 3-methylene isomer of diketene, **III**, would be formed, too. However, in this reaction, the two products are thermodynamically disfavored as their reaction energies exceed 14 kcal/mol (Chart 1, Table S3). Moreover, the activation barriers exceed 60 kcal/mol, although the barrier toward **I** is a bit lower than that toward **III**. Despite the theoretical predictions, the isomer **III** was obtained as a product of CO_2 cycloaddition to allene under a high pressure of H_2 and in the presence of $[RhCl(C_2H_4)(P^iPr_3)]_2$ as catalyst[27] (which itself usually breaks the symmetry of the reagents).

The geometries of transition state structures TS_A(**I**) and TS_A(**III**) (Figure 1) are suggestive of concerted and synchronous pathways as the distance differences between the newly created *σ*(C−C) and *σ*(C−O) bonds are much smaller than those for path B. However, in the products **I** and **III**, the *σ*(C−O) is shorter than the *σ*(C−C) distance, whereas the opposite relation is observed to hold for the TS_A(**I**) and TS_A(**III**) structures. Thus, to form *σ*-bonds on the way from the TS to the ground state of the product, the C2 and C3 atoms traverse a shorter distance than the C4 and O1 atoms do. This means that actually the process is asynchronous. TS_A(**I**) is rather slightly nonplanar, whereas TS_A(**III**) is planar, and as shown in The [2 + 2] Cycloaddition Mechanisms section they are both pericyclic.

Allene Addition to CS_2 vs Thioketene Dimerization. The energetics of thioketene dimerization is quite different from that of ketene. First, all reactions are exoergic with reaction energies of at least −14 kcal/mol (Chart 2, Tables S4 and S9). Second, the lowest activation barrier in the H_2CCS dimerization is by ca. 10 kcal/mol lower than the lowest one in the H_2CCO dimerization, and the highest is equal to 35 kcal/mol only, whereas in the ketene dimerization it is as high as 90 kcal/mol. We think that the HOMO−LUMO energy gap, smaller for the thioketene than for the ketene dimerization (Table S2), can be an explanation for the barrier lowering.

The MP2 energies for TS_B(**IX**) and TS_B(**XII**) are very close to each other (Chart 2, Tables S4 and S9). Therefore, we checked their G3 energies as well as the G3 energy for TS_B(**XIV**). Unexpectedly, the latter appeared to be the lowest, whereas this was not the case in the MP2 calculations. Similarly to the ketene dimerization reaction, differences between the MP2 and G3 calculated energies of TSs are significant and reach ca. 8 kcal/mol. There may be two main reasons for such a discrepancy: one is the unsaturation of the basis set used, and the second could be the spin−orbit coupling correction present in the G3 scheme and absent in the direct MP2 calculations.

According to the MP2 calculations, the most stable product of the thioketene dimerization is the disulfur analogue of diketene, **IX**, which is favored both thermodynamically and kinetically (Chart 2, Tables S4 and S9). Despite the fact that **XII** is not so stable as **IX**, its activation barrier is as low as that of **IX**. Thus, **XII** can possibly be formed owing to kinetic control. Surprisingly, although the product **XIV** (3,4-dimethylene-[1,2]-dithietane), with the two neighboring sulfur atoms in the ring, is the least stable product, its activation barrier (21.8 kcal/mol) is comparable with the lowest barriers: TS_B(**IX**) and TS_B(**XII**) (for IRC profiles, see Figure S2). The remaining activation barriers are higher than 29 kcal/mol. Unexpectedly, TS_B(**X**) and TS_B(**XI**) have the same energy. This is not an accident, because they are mirror images: the deformation angle of the ring, ω, is equal to 58° in TS_B(**X**) whereas in TS_B(**XI**) it is −58° (Figure 2). It is not quite obvious why this is so. The structure of TS_B(**XI**) does not look like one that has converged to the **XI** product; however, similar TS geometries were obtained by using both the MP2 and G3 models. Thus, we think that, in the course of the reaction between the TS_B(**XI**) and **XI**, rotation around the newly forming C3−C2 bond must have occurred.

Considering the possible mechanisms of thioketene dimerization, we may state that the reactions are concerted and nonsynchronous because they proceed through highly asymmetric transition state structures. In each TS_B structure, the difference between the two newly forming bond distances equals at least 0.8 Å (Figure 2). Even TS_B(**XIII**) is not an exception, though it was expected to be as symmetric as the analogous TS_B(**VI**) structure leading to 1,3-dioxetane (Figure 1). The differences in the symmetry of TS_B(**XIII**) (2,4-dimethylene-[1,3]-dithietane) and TS_B(**VI**) (2,4-dimethylene-[1,3]-dioxetane) are due to differences between the approach of the two ketene and two thioketene molecules. The former come near each other in the antiparallel manner, whereas the arrangement of the latter is antiparallel; however, the plane in which one molecule is contained is rotated through the right angle toward the other plane (Figures 1 and 2). As a result, the ring deformation angle in the former case is equal to ca. 25°, whereas in the latter case it is 0°. Note that in two cases, viz., TS_B(**XIII**) and TS_B(**XIV**), one bond has been formed almost completely as being practically equal to those in the appropriate respective products (Table S8). Ring deformation in TS_B(**XIV**) (3,4-dimethylene-[1,2]-dithietane) is significant ($\omega = -62°$), as compared to zero in TS_B(**VII**)—the oxygen analogue of **XIV**.

In the cycloaddition of allene with CS_2, reaction path A, only two products are plausible and their predicted reaction energies are equal to ca. −5 and −3 kcal/mol for **VIII** and **IX**, respectively (Chart 2). The 3-methylene isomer, **VIII**, is favored over **IX** thermodynamically; however, its activation barrier is higher by ca. 4 kcal/mol than that for the 4-methylene isomer (Figure S2). Therefore, the latter could perhaps be obtained due to kinetic control. Nevertheless, a catalyst seems to be necessary because the activation barriers exceed 50 kcal/mol and rapid reactions are hardly possible. Similarly to the TS structures found in the allene and CO_2 cycloadditions, the TS_A(**VIII**) structure is almost planar, whereas TS_B(**IX**) is deformed. The 4-methylenethietane-2-thione TS structure, TS_A(**IX**), is much more skewed than is its oxygen analogue, TS_A(**I**): 70° vs 20°, respectively. It suggests that, similarly as for diketene, in the course of the reaction leading to **IX**, the molecules approach each other perpendicularly, and the reaction is nonsynchronous. The σ(C−C) distance in TS_A(**IX**) is close to that in the product (a matter of 0.15 Å; Table S8).

Allene Addition to OCS vs Ketene Addition to Thioketene. Because the OCS molecule comprises three different atoms, the number of possible products in the course of the [2 + 2] cycloaddition with allene is greater than that for analogous reactions of the CX_2 molecules. The same holds true for the [2 + 2] cycloaddition of ketene and thioketene. Thus, four different four-membered-ring products can possibly be formed by OCS and allene reaction (**XV**, **XVI**, **XX**, and **XXI)** and eight in ketene addition to thioketene (**XVI**, **XVII**, **XVIII**, **XIX**, **XX**, **XXII**, **XXIII**, and **XXIV)** (Figure 3).

Among the eight products formed possibly in the course of the [2 + 2] cycloaddition of ketene and thioketene, three of them, namely **XXII**, **XXIII**, and **XXIV**, may be formed in endoergic reactions, whereas the remaining five may be formed in exoergic reactions (Chart 3, Tables S5 and S11). Note that the products in which the oxygen atom is built into the ring are positioned relatively high on the energy scale. Moreover, the two products that have both heteroatoms built into the ring (**XXIII**, **XXIV**) are the least stable. On the other hand, the most stable molecule **XVI** has the diketene skeleton in which the sulfur atom replaced the oxygen in the ring. Furthermore, **XVI** is the most favored because of the lowest energy barrier (21 kcal/mol; Chart 3, Tables S5 and S11). As for the thioketene dimerization reaction, the next lowest activation barrier is that toward **XVIII** (Figure S3), i.e., the product in which two heteroatoms are bound to the cyclobutane ring and are in the trans position. Also, 2-methylene-3-thietanone **XVII**, an analogue of **X**, is the second most stable compound; however, as before, the barrier toward it is higher.

The transition state structures of the ketene−thioketene cycloadditions show the processes to be concerted, yet highly asynchronous (Figure 3, Table S10). Again, generally the σ(C−C) bond is formed first and either the σ(C−O) or the σ(C−S) bond is constituted next. In one case, however, the asynchronous pathway is not so obvious, because in TS_B(**XXIII**) the proportions of the C−O and C−S distances are similar to those in the product. TS_B(**XVII**) and TS_B(**XXII**) look quite similar. Indeed, in these structures the σ(C−C) bond is almost formed and next either σ(C−O) or σ(C−S) is going to be constituted. However, in TS_B(**XVII**) (with the C−S bond), the C2−C3 distance is greater by 0.2 Å than that in TS_B(**XXII**), leading to a molecule with a much shorter C−O bond in the ring. Furthermore, in TS_B(**XVII**), the C−S distance is even shorter than the C−O distance. Similarly to the thioketene dimerization, we found two different TS structures, TS_B(**XVII**)

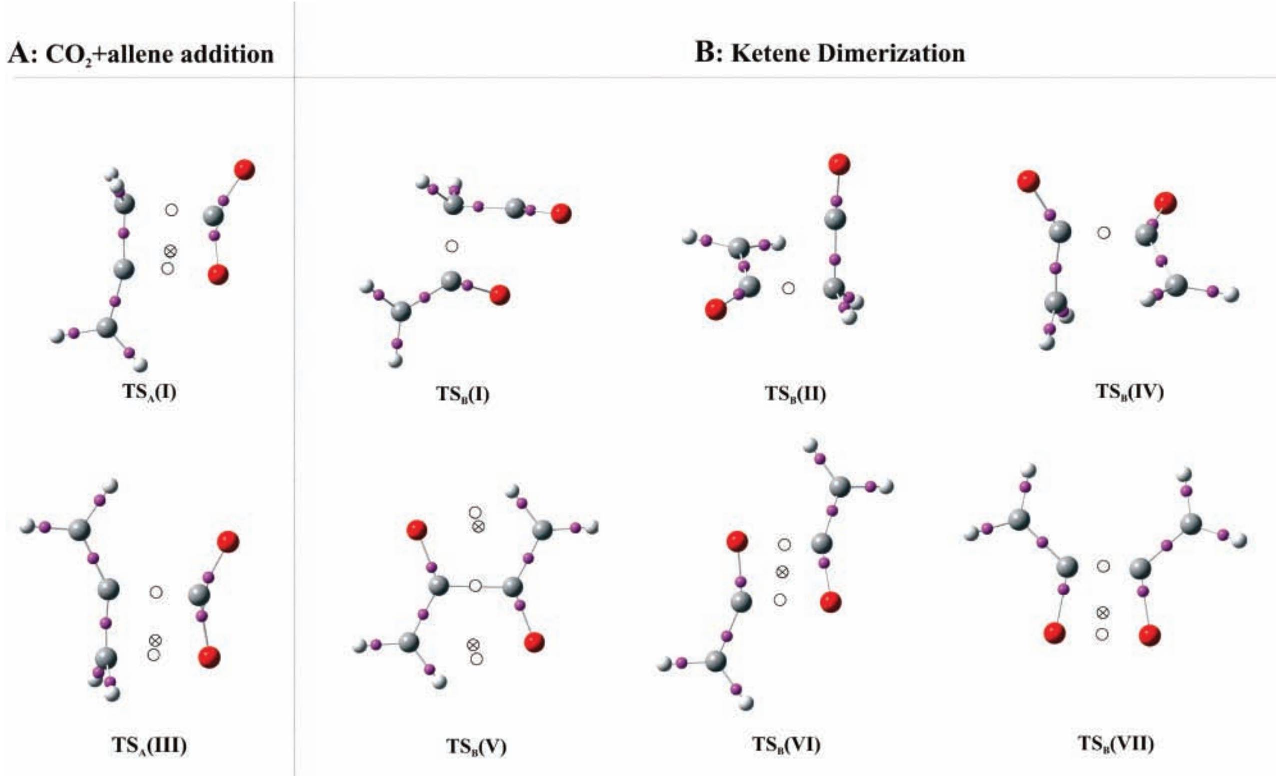

Figure 4. AIM analysis of the transition state structures for allene−CO_2 (path A) and ketene dimerization (path B) reactions calculated at the MP2/aug-cc-pVDZ level. The bond critical points (3,−1) are shown as either small balls (ordinary bonds) or open circles (newly formed bonds). The ring critical points (3,+1) are shown as crossed open circles.

and TS_B(**XIX**), of the same energy. As previously, this is due to mirror symmetry of these TS structures.

Only two, out of four, cycloaddition products formed by allene with OCS, carrying the S-atom built into the ring, seem to be thermodynamically stable. Yet their stability is as small as ca. 1 kcal/mol (Chart 3, Tables S5 and S11). Although energetic differences less than 1 kcal/mol are hardly interpretable, the energetic order of the structures with the S-atom in the ring, **XV** and **XVI**, is the same as for the analogous compounds **VIII** and **IX**, and the opposite order of TS_A(**XV**) and TS_A(**XVI**) (Figure S3) reflects also the same tendency as for TS_A(**VIII**) and TS_A(**IX**). On the other hand, the **XX** and **XXI** molecules, which have the O-atom built into the ring, exhibit an energetic order analogous to the allene with CO_2 cycloaddition products. This holds true for the TS_A(**XX**) and TS_A(**XXI**) structures, too.

As for the allene−CX_2 reactions, the TS leading to the 3-methylene isomers, TS_A(**XV**) and TS_A(**XXI**), are almost planar, whereas those leading to the 4-methylene isomers, TS_A(**XVI**) and TS_A(**XX**), exhibit nonplanarity which is more pronounced in compounds with the S-atom than in those with the O-atom built into the ring. As before, the TS_A structures indicate that the reaction path A is concerted and nonsynchronous. Also, inspection into the imaginary frequency interpretation (Table S5) confirms a simultaneous formation of the two bonds in the transition state structure along the reaction coordinate.

Summary of the Reaction Energetics. Comparison of the reaction energies and activation barrier heights in the systems studied (Charts 1−3) allows us to conclude that the reactions of the allene molecule proceed through very high activation barriers and the products are thermodynamically stable very rarely: only the products that involve the sulfur atom built into the ring are stabilized slightly (−0.7 to −5.1 kcal/mol). In the allene reactions, the lowest activation barriers occur in the case of [2 + 2] cycloaddition with CS_2 and the highest in the case of CO_2 addition. The lowest activation barriers in dimerization of ketene or thioketene are in the range of 20−30 kcal/mol. Thus, these reactions run quite easily. It is noticeable that the more oxygen atoms participate in the reaction the higher is the barrier. The energy barrier tends to change in line with the HOMO−LUMO energy gap changes (Table S2). Note that the energy gaps of allene reactions are usually by ca. 2 eV larger than those for the (thio)ketene reactions. The products possibly formed in the reactions involving ketene and thioketene are thermodynamically stable, especially those that incorporate the sulfur atom in the ring.

Inspecting the allene molecule addition energetics allows us to summarize the results as follows:

(i) Among the products incorporating the S-atom built into the ring, the 3-methylene isomers are thermodynamically more stable than the 4-methylene isomers, whereas the energetic order of the activation barriers is opposite.

(ii) Among the products incorporating the O-atom built into the ring, the 4-methylene isomers are both thermodynamically and kinetically more stable than the 3-methylene isomers.

In the reactions of (thio)ketene we observe again higher stabilities of the four-membered-ring products with the S-atom built into the ring. In this class of reactions, the most stable products are those that have a diketene skeleton which generally have the lowest activation barriers, too. In one case, however, the barrier height is lower for the diketene-like transition state, i.e., 1,3-cyclobutanedione (TS_B(**II**)). Its sulfur analogues have barriers as low as those for diketene-like analogues, **XII** and **XVIII**; however, they are thermodynamically less stable.

Summary of the TS Geometries. Several regularities can be found in the TS geometries for the subseries of analogues (Figures 1−3).

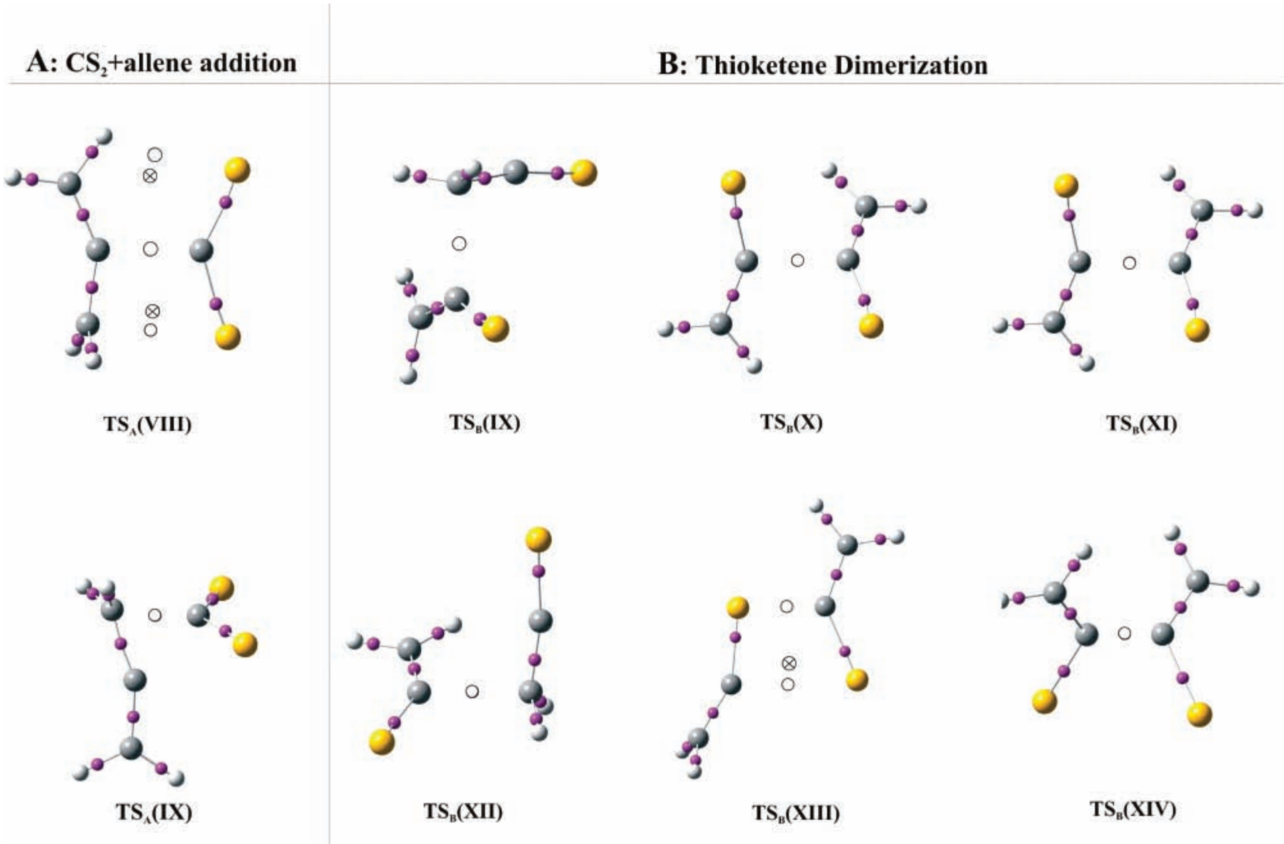

Figure 5. AIM analysis of the transition state structures for allene−CS_2 (path A) and thioketene dimerization (path B) reactions calculated at the MP2/aug-cc-pVDZ level. The bond critical points (3,−1) are shown as either small balls (ordinary bonds) or open circles (newly formed bonds). The ring critical points (3,+1) are shown as crossed open circles.

(i) The TSs leading to 3-methylene products (**III**, **VIII**, **XV**, and **XXI**) along reaction path A (XCY + allene; X, Y = O, S), are nearly planar: the ω angle does not exceed 5°.

(ii) The TSs leading to 4-methylene products (**I**, **XX**, **XVI**, **IX**) along reaction path A are nonplanar, and the ring deformation increases from 20° (CO_2), through 36° (OCS, O in the ring) or 45° (OCS, S in the ring), to 74° (CS_2).

(iii) The TSs leading to 4-methylene products (**I**, **XX**, **XVI**, **IX**) along reaction path B ($H_2CCX + H_2CCY$; X, Y = O, S) are nonplanar as well, and the ring deformation ω increases from −54° (O−C═O), through +58° (O−C═S, O in the ring) or 101° (S−C═O, S in the ring), to 106° (S−C═S).

(iv) The TSs leading to cyclobutane ring substituted with heteroatoms at the trans position (**II**, **XVIII**, **XII**) obtained along path B are nonplanar again; however, the deformation angle increases only very slightly from 45° (O═; ═O), through 48° (O═; ═S), to 51° (S═; ═S).

(v) The TSs leading to cyclobutane ring substituted with heteroatoms at the cis position (**IV**, **XIX**, **XI**) obtained along path B are nonplanar, and the ω angle increases from −61° (O═; ═O), through 111° (O═; ═S), to 122° (S═; ═S).

(vi) The TSs leading to rings with two heteroatoms built in the 1,3-positions (**VI**, **XXIII**, **XIII**) (path B) are slightly nonplanar, and the ω angle increases from −24° (−O−; −O−), through −14° (−O−; −S), to 0° (−S−; −S).

(vii) There is a decreasing trend in the ω angle for the subseries of TSs with the two heteroatoms built into the ring in the 1,2-positions (**VII**, **XXIV**, **XIV**) (path B): 0° (−O−O−), 11° (−O−S−), and −62° (−S−S-).

(viii) The tendency is not so regular for the TSs toward 2-methylene products (**V**, **XXII**, **XVII**, **X**). The ω angle changes from 0° (−O−; ═O), through 13° (−O−; ═S), to 73° (−S−; ═O), to 58° (−S−; ═S).

The [2 + 2] Cycloaddition Mechanisms. The following assumptions and reasons form the platform for our considerations of the reaction mechanism. We assumed the reactants to be in the fundamental singlet states, excluding simultaneously excitation of one of the reactants as a driving force for the reaction. When studying the reaction paths, we searched for more than one TS (required for the reaction to be two step or multistep). However, we always ended up with one TS. Although in performing the unrestricted MP2 calculations we looked for triplet TSs, we have never found one: all the optimizations of a TS structure in a triplet state either did not converge or converged to the products in their triplet states. Finally, some authors considered zwitterionic TSs;[39] however, inspection into the partial charge distribution (fitted to the electrostatic potential)[40] shows more than a two-center charge separation in the TSs. According to the above assumptions and argumentation, the reaction mechanisms considered are in the frame of concerted (one-step) reactions with the singlet TS structures.

The Woodward−Hoffmann rules[14] refer to symmetry of the reactants, symmetry of HOMO−LUMO orbitals, and their conservation throughout the reaction. The vast majority of the TSs studied show the reactions to be concerted and asynchronous. For all the TSs studied we performed AIM analysis of the electron density and found all the bond critical points (3,−1) and the ring critical point (3,+1). We stress that the present analysis yields an electron density picture for pericyclic and pseudopericyclic reactions that does not use the orbital-base picture of bonding. We made the assumption that

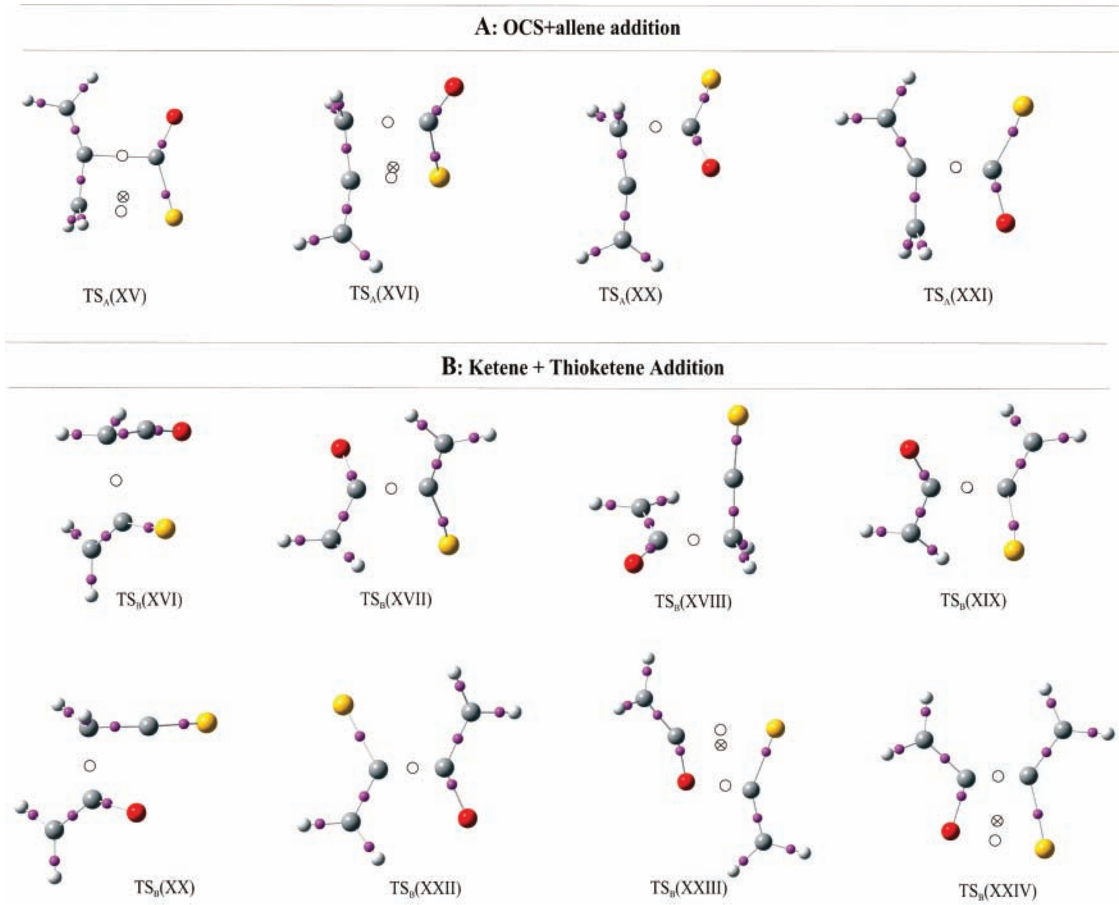

Figure 6. AIM analysis of the transition state structures for allene−OCS reaction (path A) and ketene addition to thioketene (path B) calculated at the MP2/aug-cc-pVDZ level. The bond critical points (3,−1) are shown as either small balls (ordinary bonds) or open circles (newly formed bonds). The ring critical points (3,+1) are shown as crossed open circles.

the presence of two new bond critical points (BCPs; in comparison to the number of BCPs in reactants), between the atoms in a TS that had to be connected by a new σ-bond, indicated a pericyclic type of [2 + 2] cycloaddition, which always was additionally confirmed by the presence of the ring critical point (RCP). On the other hand, the presence of only one new BCP (always accompanied by the absence of an RCP) suggested a pseudopericyclic type of the reaction. The next problem appears, however. Only some of the TSs are planar as needed for the reaction to be classified as pseudopericyclic.[20b] The reactions with TSs that are nonplanar and exhibit discontinuity can be classified as neither pericyclic nor ordinary pseudopericyclic. The latter type of the reaction we call here the nonplanar-pseudopericyclic (NP-pseudopericyclic) reaction. Now another (smaller) problem arises: which TS ring nonplanarity is sufficient for the reaction to be classified as NP-pseudopericyclic? Some authors classified the reaction with TS nonplanarity of ca. 30° as pseudopericyclic.[23d] Here, we arbitrarily accept the TS nonplanarity from −45° to +45° for the reaction to be classified as pseudopericyclic, and thus the NP-pseudopericyclic is the reaction with the discontinuity and ring nonplanarity over 45°. Last, but not least, in two cases (namely TS_B(**V**) and TS_A(**VIII**)), the new BCP and RCP indicate hydrogen-bond-like interaction[41] in the TS rather than σ-bond formation. Those critical points were ignored in the classification of the reaction mechanism.

Following the above argumentation, the allene cycloadditions with the X═C═Y molecules to the most stable products, **I**, **VIII**, and **XV** are pericyclic (Figures 4−6). The pericyclic mechanism is also revealed for the reactions through TS_A(**III**) and TS_A(**XVI**) (Figures 4−6). On the other hand, reaction path A is pseudopericyclic for **XX** and **XXI**, because the TS_A(**XX**) and TS_A(**XXI**) exhibit ring deformation smaller than 45°. Finally, the cycloadditions toward **IX** are NP-pseudopericyclic, since for the lowest barrier at path A, TS_A(**IX**), the ring deformation angle is equal to −73.6°.

Generally, the (thio)ketene cycloadditions can be classified as NP-pseudopericyclic. Indeed, TS_B(**I**), TS_B(**II**), TS_B(**IV**), TS_B(**IX**), TS_B(**X**), TS_B(**XI**), TS_B(**XII**), TS_B(**XIV**), TS_B(**XVI**), TS_B(**XVII**), TS_B(**XVIII**), TS_B(**XIX**), and TS_B(**XX**) are very nonplanar and possess only one additional BCP. In particular, reactions toward the most stable products and through the lowest barriers **II**, **IX**, and **XVI** are NP-pseudopericyclic. The other cycloadditions at path B, but toward **V** and **XXII**, are pericyclic. Indeed, each of TS_B(**VI**), TS_B(**VII**), TS_B(**XIII**), TS_B(**XXIII**), and TS_B(**XXIV**) exhibits two new BCPs and one RCP (Figures 4−6). TS_B(**XXII**) is nearly planar and exhibits only one additional BCP; thus the reaction is pseudopericyclic. TS_B(**V**) is an exception because three new BCPs and two RCPs appear. However, two of the BCPs and both RCPs are due to hydrogen-bond-like interaction in the transition state. As only one of the new BCPs corresponds to the newly formed σ-bond and the TS structure is planar, the reaction can be classified as pseudopericyclic.

Conclusions

A comprehensive theoretical MP2/aug-cc-pVDZ study was performed on the [2 + 2] cycloaddition of allene with XCY as well as H_2CCX with H_2CCY (X, Y = O, S) leading to all possible four-membered products. Attention has been focused especially on the transition state structures and energetics. It has been established that the reactions of the allene molecule proceed through very high activation barriers and the products are thermodynamically stable when the S-atom is built into the four-membered ring. Several products are possible when the H_2CCX molecule is cycloadded to the H_2CCY one; however, some of the reactions (for example, toward 4-methylene-2-oxetanone, 1,3-cyclobutanedione, 4-methylenethietane-2-thione, 1,3-cyclobutanedithione, or 4-methylenethietan-2-one) are predicted to run easily, i.e., with activation energies of ca. 20−30 kcal/mol. Generally, for the two kinds of reactions the more oxygen atoms participate in the reaction the higher is the barrier. The energy barrier tends to change in line with the HOMO−LUMO reactant energy gap changes. Except for planar TS structures leading to the 3-methylene products, during the reaction of the allene with XCY, most of the TSs are nonplanar. Generally, the more sulfur atoms participate the more nonplanar the TS is. All the studied reactions are concerted and asynchronous. The AIM analysis of the electron density distribution in the TS structures allowed distinguishing pericyclic from pseudopericyclic from nonplanar-pseudopericyclic types of reaction.

Acknowledgment. Grant G19-4 from the Interdisciplinary Center of Mathematical and Computer Modeling (ICM) of Warsaw University is gratefully acknowledged for a generous allotment of computer time. This work was financially supported by the ICRI (Warsaw) within the framework of statutory activity.

Supporting Information Available: Table S1, schematic structures, molecule numbering, and names of the system studied. Table S2, HOMO−LUMO energy gaps for the reactants. Tables S3−S11, detailed MP2/aug-cc-pVDZ calculated geometries as well as MP2/aug-cc-pVDZ energies, energies corrected for ZPE, and Gibbs free energies for all products and appropriate transition structures considered in this paper. Figures S1−S3, IRC profiles for reactions toward the most stable products. This material is available free of charge via the Internet at http://pubs.acs.org.

References and Notes

(1) Katritzky, A. R.; Rees, C. W.; Scriven, E. F. V. Four-membered rings, with all fused systems containing four-membered rings. In *Comprehensive Heterocyclic Chemistry II*; Padwa, E., Ed.; Elsevier Science: New York, 1996; Vol. 1B.

(2) (a) Clemens, R. J.; Diketene, *Chem. Rev.* **1986**, *86*, 241. (b) Clemens, R. J.; Witzeman, J. W. *Chem. Ind. (London)* **1993**, *49*, 173.

(3) Dejaegher, Y.; Kuz'menok, N. M.; Zvonok, A. M.; De Kimpe, N. The chemistry of azetidin-3-ones, oxetan-3-ones, thietan-3-ones. *Chem. Rev.* **2002**, *102*, 29−60.

(4) (a) Hirschmann, R.; Bailey, G. A.; Poos, G. I.; Walker, R.; Chemerda, J. M. A Contribution to the Chemistry of Steroid 17,21-Oxides, *J. Am. Chem. Soc.* **1956**, *78*, 4814. (b) Rowland, A. T.; Bennett, P. J.; Shoupe, T. S. The Synthesis and characterization of ring-B cholestane-3-oxetanones. *J. Org. Chem.* **1968**, *33*, 2426−2436. (c) Hanna, R.; Maalouf, G.; Muckensturm, B. *Tetrahedron* **1973**, *29*, 2297. (c) Pons, M.; Simons, J. J.; Facile, high-yield synthesis of spiro C-17-steroidal oxetan-3′-ones. *J. Org. Chem.* **1981**, *46*, 3262−3264. (d) Upjohn, Co. Br. Patent 869,564, 1959.

(5) Wojtowicz, J. A.; Polak, R. J. 3-Substituted oxetanes. *J. Org. Chem.* **1973**, *38*, 2061−2066.

(6) (a) Sweeny, W.; Wilmington; Casey, D. J.; Ford, C. Propiothiolactone Polymers. U.S. Patent 3,367,921, 1968. (b) Adams, R. D.; Huang, M.; Huang, W.; Queisser, J. A. Catalytic Cyclo-oligomerization of β-Propiothiolactone by a Dirhenium Complex. A Convenient Route to New Polythiolactone Macrocycles. *J. Am. Chem. Soc.* **1996**, *118*, 9442−9443.

(7) Karukstis, K. K.; van Hecke, G. R. Connections to Recreation, Why Do Light Sticks Glow? In *Chemistry Connections, The Chemical Basis of Everyday Phenomena*, 2nd ed.; Academic: San Diego, 2003; pp 23−28.

(8) (a) Kricka, L. J. Clinical applications of chemiluminescence. *Anal. Chim. Acta* **2003**, *500*, 279−286. (b) Beck, S., Nonradioactive detection of DNA using dioxetane chemiluminescence. *Methods Enzymol.* **1992**, *216*, 143−153. (c) Bronstein I.; et al. Chemiluminescent Detection of DNA and Protein with CDP and CDP-Star 1,2-Dioxetane Enzyme Substrates. *Bioluminescence and Chemiluminescence: Fundamentals and Applied Aspects*; Campbell, A. K., Kricka, L. J., Stanley, P. E., Eds.; John Wiley: Chichester, UK, 1994; pp 269−272. (d) Voyta, J. C.; et al. Chemiluminescent Detection of Glycosidic Enzymes with 1,2-Dioxetane Substrates. *Bioluminescence and Chemiluminescence: Molecular Reporting with Photons*; Hastings, J. W., Kricka, L. J., Stanley, P. E., Eds.; John Wiley: Chichester, UK: 1997; pp 529−532. (e) http://www.devicelink.com/ivdt/archive/01/04/002.html. (f) http://lanthanides.tripod.com/ln-cl.html.

(9) (a) Surh, Y. J.; Kim, S. G.; Liem, A.; Lee, J. W.; Miller, J. A. Inhibitory effects of isopropyl-2-(1,3-dithietane-2-ylidene)-2-[N-(4-methylthiazol-2-l)carbamoyl]acetate (YH439) on benzo[α]pyrene-induced skin carcinogenesis and micronucleated reticulocyte formation in mice. *Mutat. Res.* **1999**, *423*, 149−53. (b) Kim, S. G.; Surh, Y. J.; Sohn, Y.; Yoo, J. K.; Lee, J. W.; Liem, A.; Miller, J. A. Inhibition of vinyl carbamate-induced hepatotoxicity, mutagenicity, and tumorigenicity by isopropyl-2-(1,3-dithietane-2-ylidene)-2-[N-(4-methylthiazol-2-yl)carbamoyl]-acetate (YH439). *Carcinogenesis* **1998**, *19*, 687−90.

(10) (a) Rice, F. O.; Greenberg, J. Ketene. II. Rate of Polymerization. *J. Am. Chem. Soc.* **1934**, *56*, 2132−2134. (b) Rice, F. O.; Roberts, R. The Structure of Diketene. *J. Am. Chem. Soc.* **1943**, *65*, 1677−1681. (c) Chickos, J. S.; Sherwood, D. E.; Jug, K. Mechanism of thermolysis of diketene in the gas phase. *J. Org. Chem.* **1978**, *43*, 1146−1150.

(11) (a) Carless, H. J. *Photochemistry in Organic Synthesis*; Coyte, J. D., Ed.; Royal Society of Chemistry: London, 1986; p 95. (b) Salzner, U.; Bachrah, S. M., Ab Initio Studies of the Dimerization of Ketene and Phosphaketene. *J. Am. Chem. Soc.* **1994**, *116*, 6850−6855. (c) Seidl, E. T.; Schaefer, H. F., III. Diketene and Its Cyclic $C_4H_4O_2$ Isomers 1,3-Cyclobutanedione and 2,4-Dimethylene-1,3-dioxide. *J. Am. Chem. Soc.* **1990**, *112*, 1493−1499. (d) Jug, K.; Chickos, J., Mechanistic Pathways for Ketene Dimerization. *Theor. Chim. Acta (Berlin)* **1975**, *40*, 207−219. (e) Jug, K.; Dwivedi, C. P. D., Reaction Pathways for Various Ketene Dimers. *Theor. Chim. Acta (Berlin)* **1978**, *90*, 249−257. (f) Fu, X. Y.; Decai, F.; Yanbo, D. Theoretical Studies on the Reaction Mechanism of Ketene Dimerization Reactions. *J. Mol. Struct. (THEOCHEM)* **1988**, *167*, 349−358. (g) Dobrowolski, J. Cz.; Jamróz, M. H.; Borowiak, M. A.; Quaranta, E.; Aresta, M. Theoretical IR and Raman spectra of diketene and its 3-methylene isomer. *Vib. Spectrosc.* **2000**, *22*, 19−28.

(12) Seidl, E. T.; Schaefer, H. F., III. Theoretical Investigations of the Dimerization of Ketene: Does the 2S + 2A Cycloaddition Reaction Exist? *J. Am. Chem. Soc.* **1991**, *113*, 5195−5200.

(13) Salzner, U.; Bachrach, S. M. Ab Initio Studies of the Dimerization of Ketene and Phosphaketene. *J. Am. Chem. Soc.* **1994**, *116*, 6850−6855.

(14) (a) Woodward, R. B.; Hoffmann, R. The Conservation of Orbital Symmetry, *Angew. Chem., Int. Ed.* **1969**, *8*, 781−932, (b) Woodward, R. B.; Hoffmann, R. *The Conservation of Orbital Symmetry*; Verlag Chemie, Weinheim and Academic Press: New York, 1970.

(15) Zhao, X.; Cai, Z.; Wang, G.; Pan, Y.; Wu, B. The conservation of generalized parity: molecular symmetry and conservation rules in chemistry. *J. Mol. Struct. (THEOCHEM)* **2002**, *586*, 209−223.

(16) (a) Lowry, T. H.; Richardson, K. S. *Mechanism and Theory in Organic Chemistry*, 3rd ed.; Harper and Row: New York 1987. (b) Jean, Y.; Volatron, F. *An Introduction to Molecular Orbitals*; Oxford University Press: New York, 1993.

(17) Bernardi, F.; Bottoni, A.; Olivucci, M.; Robb, M. A.; Schlegel, H. B.; Tonachini, G. Do Supra-Antra Paths Exist for 2+2 Cycloaddition Reactions? Analytical Computation of the MC-SCF Hessians for Transition States of C_2H_2 with C_2H_2, Singlet O_2, and Ketene. *J. Am. Chem. Soc.* **1988**, *110*, 5993−5995.

(18) Zimmerman, H. E. *Pericyclic Reactions*; Marchand, A. P., Lehr, R. E., Eds.; Academic Press: New York, 1977.

(19) (a) Ross, J. A.; Seiders, R. P.; Lemal, D. M. An Extraordinary Facile Sufoxide Automerization. *J. Am. Chem. Soc.* **1976**, *98*, 4325−4327. (b) Bushweller, C. H.; Ross, J. A.; Lemal, D. M. Autoimerization of a Dewar Thiophene and Its *exo*-S-Oxide. A Dramatic Contrast. *J. Am. Chem. Soc.* **1977**, *99*, 629−631.

(20) (a) Birney, D. M.; Wagenseller, P. E. An ab Initio Study of the Reactivity of Formylketene. Pseudopericyclic Reactions Revisited. *J. Am. Chem. Soc.* **1994**, *116*, 6262−6270. (b) Birney, D. M.; Ham, S.; Unruh, G. R.; Pericyclic and Pseudopericyclic Thermal Cheletropic Decarbonylations: When Can a Pericyclic Reaction Have a Planar, Pseudopericyclic Transition State? *J. Am. Chem. Soc.* **1997**, *119*, 4509−4517. (c) Birney, D. M. Electrocyclic Ring Openings of 2-Furylcarbene and Related Carbenes: A Comparison between Pseudopericyclic and Coarctate Reactions. *J. Am. Chem. Soc.* **2000**, *122*, 10917−10925. (d) Shumway, W.; Ham, S.; Moer, J.; Whittlesey, B. R.; Birney, D. M. Felkin-Anh Stereoselectivity in Cycloadditions of Acetylketene: Evidence for a Concerted, Pseudopericyclic Pathway. *J. Org. Chem.* **2000**, *65*, 7731−7739. (e) Zhou, C.; Birney, D. M. A Density Functional Theory Study Clarifying the Reactions of Conjugated Ketenes with Formaldimine. A Plethora of Pericyclic and Pseudopericyclic Pathways. *J. Am. Chem. Soc.* **2002**, *124*, 5231−5241. (f)

Wei, H.-X.; Zhou, C.; Ham, S.; White, J. M.; Birney, D. M. Experimental Support for Planar Pseudopericyclic Transition States in Thermal Cheletropic Decarbonylations. *Org. Lett.* **2004**, *6*, 4289−4292.

(21) (a) Fabian, W. M. F.; Bakulev, V. A.; Kappe, C. O.; Pericyclic versus Pseudopericyclic 1,5-Electrocyclization of Iminodiazomethanes. An ab Initio and Density Functional Theory Study. *J. Org. Chem*. **1998**, *63*, 5801−5805. (b) Fabian, W. M. F.; Kappe, C. O.; Bakulev, V. A. Ab Initio and Density Functional Calculations on the Pericyclic vs Pseudopericyclic Mode of Conjugated Nitrile Ylide 1,5-Electrocyclizations. *J. Org. Chem.* **2000**, *65*, 47−53. (c) Fukushima, K.; Iwahashi, H.; Natural Bond Orbital Analysis of Pericyclic and Pseudopericyclic 1,5-Electrocyclizations of Conjugated Nitrileimines. *Bull. Chem. Soc. Jpn.* **2004**, *77*, 1671−1679.

(22) Cabaleiro-Lago, E. M.; Rodríguez-Otero, J.; Hermida-Ramón, J. Evaluation of Magnetic Properties as a Criterion for the Elucidation of the Pseudopericyclic Character of 1,5-Electrocyclizations in Nitrile Ylides. *J. Phys. Chem. A* **2003**, *107*, 4962−4966.

(23) (a) Rodríguez-Otero, J.; Cabaleiro-Lago, E. M.; Hermida-Ramón, J.; Peña-Gallego A.; DFT Study of Pericyclic and Pseudopericyclic Thermal Cheletropic Decarbonylations. Evaluation of Magnetic Properties. *J. Org. Chem.* **2003**, *68*, 8823−8830. (b) Montero-Campillo, M. M.; Rodríguez-Otero, J.; Cabaleiro-Lago, E. M. Ab Initio and DFT Study of the Reaction Mechanism of Diformylketene with Formamide. *J. Phys. Chem. A* **2004**, *108*, 8373−8377. (c) Peña-Gallego A.; Rodríguez-Otero, J.; Cabaleiro-Lago, E. M. A DFT Study of the Boulton-Katritzky Rearrangement of (5*R*)-4-Nitrosobenz[*c*]isoxazole and Its Anion: Pseudopericyclic Reactions with Aromatic Transition States. *J. Org. Chem*. **2004**, *69*, 7013−7017. (d) Cabaleiro-Lago, E. M.; Rodríguez-Otero, J.; González-López, I.; Peña-Gallego A.; Hermida-Ramón, J. A DFT Study of the Pericyclic/Pseudopericyclic Character of Cycloaddition Reactions of Ethylene and Formaldehyde to Buta-1,3-dien-1-one and Derivatives. *J. Phys. Chem. A* **2005**, *109*, 5636−5644.

(24) Chamorro, E. The nature of bonding in pericyclic and pseudopericyclic transition states: Thermal chelotropic decarbonylations. *J. Chem. Phys.* **2003**, *118*, 8687−8698.

(25) Silva López, C.; Nieto Faza, O.; Cossio, F. P.; York, D. M.; de Lera, A. R.; Ellipticity: A Convenient Tool To Characterize Electrocyclic Reactions. *Chem.*−Eur. J. **2005**, *11*, 1734−1738.

(26) (a) Dobrowolski, J. Cz.; Jamróz, M. H.; Borowiak, M. A.; Quaranta, E.; Aresta, M. Theoretical IR and Raman spectra of diketene and its 3-methylene isomer. *Vib. Spectrosc.* **2000**, *22*, 19−28. (b) Rode, J. E.; Dobrowolski, J. Cz.; Borowiak, M. A. Theoretical study on stability and NMR chemical shifts of the diketene molecule, its isomers and their mono- and disulphur analogues. *J. Mol. Struct. (THEOCHEM)* **2001**, *545*, 233−254. (c) Rode, J. E.; Dobrowolski, J. Cz.; Jamróz, M. H.; Borowiak, M. A. Theoretical IR spectra of the diketene molecule its isomers and their mono- and disulphur analogues. *J. Mol. Struct.* **2001**, *565*−*566*, 433−438.

(27) Aresta, M.; Dibenedetto, A.; Papai, I.; Schubert, G. Unprecedented formal '2+2' addition of allene to CO_2 promoted by $[RhCl(C_2H_4)(P^iPr_3)]_2$: direct synthesis of the four membered lactone α-methylene-*β*-oxiethanone. The intermediacy of $[RhH_2Cl(P^iPr_3)]_2$: theoretical aspects and experiments. *Inorg. Chim. Acta* **2002**, *334*, 294−300.

(28) Ma, N. L.; Wong, M. W.; A Theoretical Study of the Properties and Reactivities of Ketene, Thioketene, and Selenoketene. *Eur. J. Org. Chem.* **2000**, 1411−1421.

(29) (a) Biegler-König, F.; Schönbohm, J.; AIM2000, A Program to Analyze and Visualize Atoms in Molecules, version 2, 2002. (b) Bader, R. F. W. *Atoms in Molecules: A Quantum Theory*; Clarendon Press: Oxford, 1990.

(30) Møller, C.; Plesset, M. S. Note on an Approximation Treatment for Many-Electron Systems. *Phys. Rev.* **1934**, *46*, 618−622.

(31) (a) Woon, D. E.; Dunning, T. H., Jr. Gaussian basis sets for use in correlated molecular calculations. III. The atoms aluminum through argon. *J. Chem. Phys.* **1993**, *98*, 1358−1371. (b) Kendall, R. A.; Dunning, T. H., Jr.; Harrison, R. J. Electron affinities of the first-row atoms revisited. Systematic basis sets and wave functions. *J. Chem. Phys.* **1992**, *96*, 6796−6806.

(32) (a) Frisch, M. J.; Trucks, G. W.; Schlegel, H. B.; Scuseria, G. E.; Robb, M. A.; Cheeseman, J. R.; Zakrzewski, V. G.; Montgomery, J. A.; Stratmann, R. E.; Burant, J. C.; Dapprich, S.; Milliam, J. M.; Daniels, A. D.; Kudin, K. N.; Strain, M. C.; Farkas, O.; Tomasi, J.; Barone, V.; Cossi, M.; Cammi, R.; Mennucci, B.; Pomelli, C.; Adamo, C.; Clifford, S.; Ochterski, J.; Petersson, G. A.; Ayala, P. Y.; Cui, Q.; Morokuma, K.; Malick, D. K.; Rabuck, A. D.; Raghavachari, K.; Foresman, J. B.; Cioslowski, J.; Ortiz, J. V.; Stefanov, B. B.; Liu, G.; Liashenko, A.; Piskorz, P.; Komaromi, I.; Gomperts, R.; Martin, R. L.; Fox, D. J.; Keith, T. A.; Al-Laham, M. A.; Peng, C. Y.; Nanayakkara, A.; Gonzales, C.; Challacombe, M.; Gill, P. M. W.; Johnson, B. G.; Chen, W.; Wong, M. W.; Andres, J. L.; Replogle, E. S.; Head-Gordon, M.; Reploge, E. S.; Pople, J. A. *Gaussian 98*, revision A.7; Gaussian, Inc.: Pittsburgh, PA, 1998. (b) Frisch, M. J.; Trucks, G. W.; Schlegel, H. B.; Scuseria, G. E.; Robb, M. A.; Cheeseman, J. R.; Montgomery, J. A., Jr.; Vreven, T.; Kudin, K. N.; Burant, J. C.; Millam, J. M.; Iyengar, S. S.; Tomasi, J.; Barone, V.; Mennucci, B.; Cossi, M.; Scalmani, G.; Rega, N.; Petersson, G. A.; Nakatsuji, H.; Hada, M.; Ehara, M.; Toyota, K.; Fukuda, R.; Hasegawa, J.; Ishida, M.; Nakajima, T.; Honda, Y.; Kitao, O.; Nakai, H.; Klene, M.; Li, X.; Knox, J. E.; Hratchian, H. P.; Cross, J. B.; Bakken, V.; Adamo, C.; Jaramillo, J.; Gomperts, R.; Stratmann, R. E.; Yazyev, O.; Austin, A. J.; Cammi, R.; Pomelli, C.; Ochterski, J. W.; Ayala, P. Y.; Morokuma, K.; Voth, G. A.; Salvador, P.; Dannenberg, J. J.; Zakrzewski, V. G.; Dapprich, S.; Daniels, A. D.; Strain, M. C.; Farkas, O.; Malick, D. K.; Rabuck, A. D.; Raghavachari, K.; Foresman, J. B.; Ortiz, J. V.; Cui, Q.; Baboul, A. G.; Clifford, S.; Cioslowski, J.; Stefanov, B. B.; Liu, G.; Liashenko, A.; Piskorz, P.; Komaromi, I.; Martin, R. L.; Fox, D. J.; Keith, T.; Al-Laham, M. A.; Peng, C. Y.; Nanayakkara, A.; Challacombe, M.; Gill, P. M. W.; Johnson, B.; Chen, W.; Wong, M. W.; Gonzalez, C.; Pople, J. A. *Gaussian 03*, revision C.02; Gaussian, Inc.: Wallingford, CT, 2004.

(33) Peng, C.; Schlegel, H. B. Combining Synchronous Transit and Quasi-Newton Methods to Find Transition States. *Isr. J. Chem.* **1993**, *33*, 449.

(34) Peng, C.; Ayala, P. Y.; Schlegel, H. B.; Frisch, M. J. Using Redundant Internal Coordinates to Optimize Equilibrium Geometries and Transition States. *J. Comput. Chem.* **1995**, *16*, 49.

(35) (a) Gonzales, C.; Schlegel, H. B. An improved algorithm for reaction path following. *J. Chem. Phys.* **1989**, *90*, 2154−2161. (b) Gonzales, C.; Schlegel, H. B. Reaction path following in mass-weighted internal coordinates. *J. Phys. Chem.* **1990**, *94*, 5523−5527.

(36) (a) Curtiss, L. A.; Raghavachari, K.; Redfern, P. C.; Rassolov, V.; Pople, J. A. Gaussian-3 theory for molecular energies of first- and second-row compound. *J. Chem. Phys.* **1998**, *109*, 7764−7776. (b) Curtiss, L. A.; Redfern, P. C.; Raghavachari, K.; Pople, J. A. Gaussian-3 Theory: A Variation Based on Third-Order Perturbation Theory and an Assessment the Contribution of Core-Related Correlation. *Chem. Phys. Lett.* **1999**, *313*, 600−607. (c) Curtiss, L. A.; Redfern, P. C.; Rassolov, V.; Kedziora, G.; Pople, J. A. Extension of Gaussian-3 theory to molecules containing third-row atoms K, Ca, Ga-Kr. *J. Chem. Phys.* **2001**, *114*, 9287−9295. (d) Curtiss, L. A.; Raghavachari, K.; Redfern, P. C.; Kedziora, G.; Pople, J. A. On Comparison of Experimental Theoretical Data with G3 Theory. *J. Phys. Chem. A* **2001**, *105*, 227−228.

(37) Flükiger, P.; Lüthi, H. P.; Portmann, S.; Weber, J. *MOLEKEL 4.0*; Swiss Centre for Scientific Computing: Manno, Switzerland, 2000.

(38) Matsumoto, M. Advanced Chemistry of Dioxetane-Based Chemiluminescent substrates originating from bioluminescence. *J. Photochem. Photobiol., C* **2004**, *5*, 27−53.

(39) Siri, D.; Gaudel-Siri, A.; Pons, J.-M.; Liotard, D.; Rajzmann, M. Reaction mechanism studies made simple using simulated annealing. Potential energy surface exploration. *J. Mol. Struct. (THEOCHEM)* **2002**, *588*, 71−78.

(40) Breneman, C. M.; Wiberg, K. B. Determining atom-centered monopoles from molecular electrostatic potentials. The need for high sampling density in formamide conformational analysis. *J. Comput. Chem.* **1990**, *11*, 361−373.

(41) (a) Sadlej-Sosnowska, N.; Dobrowolski, J. Cz.; Oziminski, W.; Mazurek, A. P. On the conformation and hydrogen bonding in the vigabatrin amino acid. *J. Phys. Chem. A* **2002**, *106*, 10554−10562. (b) Wojtulewski, S.; Grabowski, S. J. Ab initio and AIM studies on intramolecular dihydrogen bonds. *J. Mol. Struct.* **2002**, *645*, 287−294.